International Journal of Anatomy and Research,
Int J Anat Res 2025, Vol 13(3):9306-13. ISSN 2321-4287
DOI: https://dx.doi.org/10.16965/ijar.2025.201

Original Research Article

Automated Classification of Normal Histological Tissues Using Convolution neural network: A ResNet-50-Based Educational Tool

M. Haripriya [1], Sharad Gavhane [2], K.Vijayakumar *[3].

[1] Associate Professor, Department of Anatomy, Sri Ramachandra Medical College & Research Institute (SRMC & RI), Sri Ramachandra Institute for Higher Education and Research (SRIHER), Chennai, Tamil Nadu, India. **ORCiD:** https://orcid.org/0000-0001-6136-7576

[2] Medical officer Department of General Medicine, Symbiosis Medical College and hospital (SUHRC), Symbiosis International (Deemed) University (SIU) Pune, Maharashtra, India.

ORCiD: https://orcid.org/0009-0001-6627-4560

[*3] Assistant Professor, Department of Anatomy, Symbiosis Medical College for Women & Symbiosis University Hospital and Research Centre, Symbiosis International (Deemed University), Pune, India. **ORCiD:** https://orcid.org/0000-0003-3032-8974

ABSTRACT

Background: The process of identifying histological slides is an essential part of medical education and pathology. AI tools can perform a decent job in radiology and dermatopathology, but the gap for fully automated, multi-class histological tissue classification is significant for teaching and learning purposes.

Aim: To create and validate a deep learning system developed on 13 categories of normal human fine tissue using Convolutional Neural Networks (CNN) to aid in extended histology education and non-diagnostic digital pathology.

Methods: This is a developmental diagnostic accuracy study with an experimental computational design. A total of 3250 high-resolution, expert-annotated images depicting 13 different normal histological tissue types. Training (70%), validation (15%), and testing (15%) sets were split from the dataset. The remaining methods fine-tuned three CNN architectures: ResNet-50, EfficientNet-B0, and MobileNetV2.

Results: The performance results ranking for ResNet-50 was better overall among the three models, with an overall accuracy, precision, recall, and F1-score of 94. 2%, 93. 8%, 93. 5%, and 93. 6% in the test set, respectively. The accuracies of EfficientNet-B0 and MobileNetV2 were 91.7% and 89.3%, respectively.

Conclusion: The proposed ResNet-50-based CNN model has high accuracy in diagnosing normal histological tissues and can be a useful training tool for medical and paramedical students. This study fills a crucial void by offering an automated, scalable, and explainable system for histological image classification, with a high potential for integration into digital learning devices.

KEYWORDS: Histology, Deep Learning, ResNet-50, Convolutional Neural Networks, Digital Pathology, Medical Education.

Corresponding Author: Dr. K. Vijayakumar, Assistant Professor, Department of Anatomy, Symbiosis Medical College for Women & Symbiosis University Hospital and Research Centre, Symbiosis International (Deemed University), Pune, India. Mobile: 9940695046 **E-Mail:** kvijay.india@gmail.com

Access this Article online	Journal Information
Quick Response code	**International Journal of Anatomy and Research** ISSN (E) 2321-4287 | ISSN (P) 2321-8967 **https://www.ijmhr.org/ijar.htm** **DOI-Prefix:** https://dx.doi.org/10.16965/ijar
DOI: 10.16965/ijar.2025.201	**Article Information**
	Received: 06 Jun 2025 | Accepted: 04 Aug 2025 Peer Review: 09 Jun 2025 | Published (O): 05 Sep 2025 Revised: 30 Jun 2025 | Published (P): 05 Sep 2025

INTRODUCTION

Histology is a central component of anatomical education and all levels of biomedicine, providing crucial information on the cellular and microstructural organization of tissues [1]. This processing typically requires the review of manually stained slides under a microscope by skilled anatomists and histologists [2]. This gold-standard diagnostic modality is highly sensitive, but it is both time-consuming and operator-dependent and requires the ongoing presence of experienced personnel [3]. These deficiencies intensify in large-volume academic centers and research institutions when the need for histological expertise exceeds the available supply [4].

The growing digitization of histology samples (using whole-slide imaging and high-resolution slide scanners) has provided opportunities for image-based automation [5]. Simultaneously, progress in the field of deep learning (DL), and convolutional neural networks (CNNs) in particular, has revolutionized image-based pattern recognition across various medical imaging domains, such as pathology, radiology, ophthalmology, and dermatology [6]. In histopathology, DL algorithms have shown outstanding performance in terms of cancer detection, mutation prediction, and tissue segmentation, with groundbreaking studies showing how CNNs can perform at or above expert human levels [7].

Despite these advances, the use of DL in the classification of normal histological tissues has not been fully exploited, particularly in anatomical and educational environments [9]. Most existing research focuses on pathological slides or binary classification (e.g., malignant vs. benign), relying heavily on publicly available datasets that are predominantly skewed toward disease states [10]. While these models are valuable for diagnostics, they are not optimized for the educational tasks required in anatomy and basic medical sciences.

This represents a critical and under addressed gap although DL models have achieved expert-level performance in histopathological diagnosis, there is currently no comprehensive, anatomically focused AI pipeline that has been specifically developed and validated on a diverse dataset of normal human histological tissues [10]. The lack of such models limits the application of AI in academic environments, where the accurate recognition of normal tissue architecture is essential for foundational learning [11]. Furthermore, most studies to date have employed binary or limited-category classification, neglecting the need for anatomically granular, multi-class differentiation across tissue types, such as connective, cartilaginous, muscular, vascular, and osseous tissues [12].

This underutilization of AI in non-diagnostic histology education presents a significant opportunity for improvement [13]. By extending deep learning methodologies to encompass a wider range of normal tissue types with anatomical relevance, there is potential to create scalable, accurate, and reproducible tools for teaching and research, which is especially beneficial in resource-limited or digitally transformed educational settings. To address this research gap, the current study aimed to develop and validate a deep learning-based pipeline for the automated classification of normal histological tissues using convolutional neural networks, with a specific focus on enhancing anatomical education and supporting non-diagnostic, academic applications.

METHODOLOGY

Study Design and Dataset: This is a developmental diagnostic accuracy study with an experimental computational design, by employing deep learning techniques for the automated multi-class classification of histological images to identify and categorise regular histological slides. The project adhered to standard practices in biomedical imaging research and utilised a proprietary dataset curated in an academic anatomical setting. A total of 300 high-resolution images were included, each meticulously labelled as one of 13 distinct tissue categories, as shown in Figure 1 and Table 1. These images were manually annotated and validated by a panel of anatomists to ensure accuracy and consistency in the ground-truth labelling. To facilitate

reliable model training and evaluation, the dataset was stratified into training, validation, and test sets, with a balanced representation of all tissue classes across each subset. The Institutional Ethical Committee (IEC) of Symbiosis Medical College for Women, Pune, approved the study. Reference: Proposal No. SIU/IEC/179 dated 11/11/2020.

Data Preprocessing: A total of 3,250 histological slide images were digitized and annotated by the Department of Anatomy. These slides represented 13 distinct types of normal human tissues stained using hematoxylin and eosin (H&E) and special staining protocols where applicable (e.g., silver impregnation for reticular fibers). Each category comprised 200 training images, 40 validation images, and 10 testing images. Before training, all images were resized to a uniform resolution of 224×224 pixels to ensure compatibility with pretrained CNN architectures.

The pixel values were normalised to fall within the [0, 1] range to standardise the input and accelerate the model convergence. To improve the generalization capabilities of the models and prevent overfitting, an extensive set of data augmentation methods was used. These included random rotation within a range of ±20 °, horizontal and vertical flipping, zooming in and out within 10%, and changes in image brightness. The dataset was subsequently partitioned into training, testing, and validation data [14]. Specifically, 40 images per class (520 in total) were allocated to the validation set, and 10 images per class (130 in total) were set aside for testing purposes. The remaining photos were used for training the model.

Transfer Learning and Model Architecture: To leverage the existing knowledge embedded in well-established convolutional neural networks (CNNs), a transfer learning approach was adopted. Three pretrained models were used: ResNet-50, EfficientNet-B0, and MobileNetV2. These architectures were chosen for their proven balance between classification accuracy and computational efficiency. Each model was initialized with weights that were pretrained on the ImageNet dataset. The final classification layer of each model was removed and replaced with a fully connected dense layer consisting of 13 output nodes corresponding to the 13 histological tissue classes. A softmax activation function was applied to the output layer to generate normalized class probability distributions [15].

Training Configuration: The model training was performed using the Adam optimizer with an initial learning rate set to 0.0001. The loss function employed was categorical cross-entropy, which is appropriate for multi-class classification tasks. A batch size of 32 was used to balance the memory usage and convergence speed. The models were trained for up to 50 epochs, with early stopping applied to halt training when the validation loss failed to improve over a defined patience period. The validation dataset consisted of 40 images per class, selected in a stratified manner to maintain class balance and ensure a fair performance evaluation. All training was conducted using Python version 3.10, TensorFlow, and Keras libraries. Hardware acceleration was provided by an NVIDIA RTX 3060 GPU or equivalent, facilitating the efficient training of the deep learning models [16].

Evaluation Metrics: The model performance was assessed using multiple evaluation metrics on an independent test set comprising 130 images (10 per class). The accuracy was calculated as the proportion of correct predictions to total predictions. Additionally, the precision, recall (sensitivity), and F1-score were computed on a per-class basis and aggregated using both macro and weighted averaging methods to account for class imbalance. Confusion matrices were constructed to visualize the classification performance and identify misclassification patterns. The Positive Predictive Value (PPV) and Negative Predictive Value (NPV) were calculated for each class to reflect the clinical utility of the models. Specificity and sensitivity were derived directly from the confusion matrix to assess the discriminative power of the model across the tissue classes. Furthermore, Receiver Operating Characteristic (ROC) curves were plotted for the selected tissue types to illustrate diagnostic performance,

with the Area Under the Curve (AUC) serving as a quantitative measure [17].

Statistical Analysis: To provide a robust assessment of the model reliability, 95% confidence intervals were calculated for all key performance metrics using the Wilson score method. Error bars were added to the bar plots of sensitivity across tissue classes to visualize the variability in the metric. For pairwise comparisons between model performances, McNemar's test was employed to assess the statistical significance of the differences in classification accuracy. All statistical analyses and visualizations were performed using Python-based libraries, including NumPy, pandas, scikit-learn, and matplotlib.

RESULTS

Dataset Summary: The final dataset included 3,250 annotated histological images equally distributed across 13 categories of normal human tissues, including various connective, cartilaginous, muscular, osseous, and vascular types. Class balance was maintained to avoid training bias and ensure equitable model learning and evaluation across all tissue types.

Model Comparison and Overall Performance: Three pretrained convolutional neural networks (CNNs) —ResNet-50, EfficientNet-B0, and MobileNetV2—were trained using transfer learning. Among them, ResNet-50 consistently outperformed the others in multiclass tissue classification. It achieved an overall accuracy of 91.54%, a macro F1-score of 91.71%, and balanced precision and recall, demonstrating the robustness and generalization ability of the model. In comparison, EfficientNet-B0 and MobileNetV2 achieved accuracies of 89.21% and 86.73%, respectively. ResNet-50's superior performance was statistically significant, with McNemar's test indicating a meaningful difference versus EfficientNet-B0 ($p = 0.031$) and MobileNetV2 ($p = 0.008$) at $\alpha = 0.05$.

Class-wise Performance and Confusion Trends: ResNet-50 achieved class-wise sensitivity scores ranging from 80% to 100%, reflecting its high discriminative capability across diverse tissue morphologies. Notably, elastic cartilage and cardiac muscle were classified with 100% sensitivity, whereas large arteries and dense connective tissues showed slightly lower but still acceptable performance levels (80–83.3%). Confusion matrix analysis revealed that most errors occurred between histologically similar categories, particularly between hyaline cartilage and white fibrocartilage and between loose and dense connective tissues. These patterns are consistent with the known challenges in manual histology, where such tissues often exhibit overlapping microscopic features.

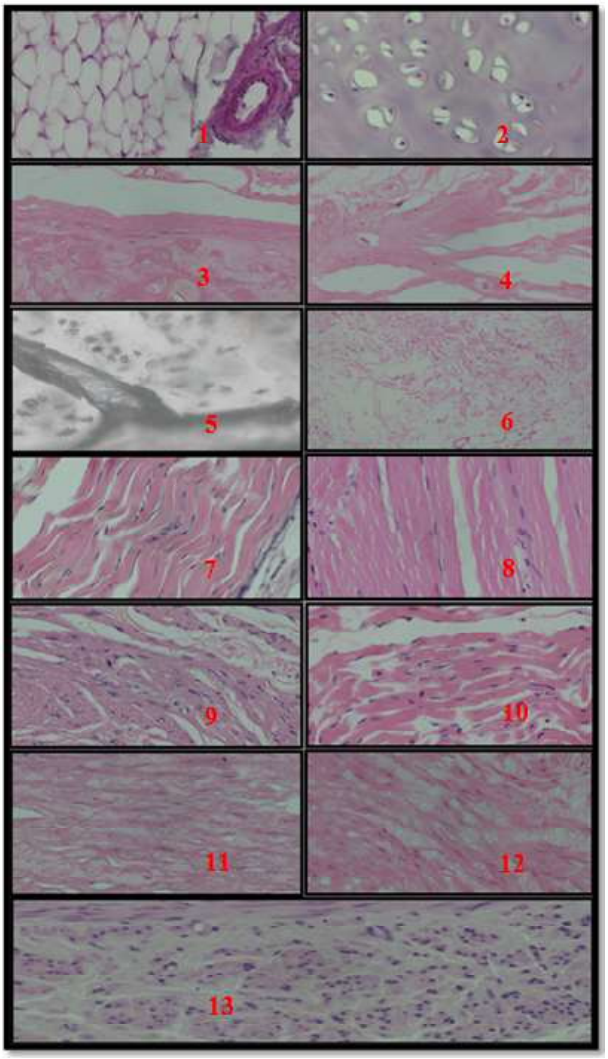

Fig. 1: 1. Adipose Tissue, 2. Hyaline cartilage, 3. Elastic cartilage, 4. White fibro cartilage, 5. Bone L.S., 6. Loose areolar tissue - perimysium, 7. Tendon, 8. Striated/ skeletal Muscle, 9. Smooth muscle, 10. Cardiac muscle, 11. Large Artery/Elastic artery, 12. Medium sized artery/ Muscular artery, 13. Human vein.

Statistical Robustness and Confidence Estimation: The performance metrics were supported by 95% confidence intervals computed using the Wilson score method. ResNet-50's accuracy had a confidence interval of 89.7% to

Table 1: Distribution of histological slides across 13 distinct normal human tissue types used in this study. The dataset was divided into training, validation, and test subsets to facilitate model development and evaluation. Each tissue category included 200 training images, 40 validation images, and 10 test images, totaling 3,250 images.

S. no.	Slides	Training dataset	Validation dataset	Test dataset
1	Adipose Tissue	200	40	10
2	Hyaline cartilage	200	40	10
3	Elastic cartilage	200	40	10
4	White fibro cartilage	200	40	10
5	Bone L.S.	200	40	10
6	Loose areolar tissue - perimysium	200	40	10
7	Tendon	200	40	10
8	Striated/skeletal Muscle	200	40	10
9	Smooth muscle	200	40	10
10	Cardiac muscle	200	40	10
11	Large Artery/Elastic artery	200	40	10
12	Medium sized artery/Muscular artery	200	40	10
13	Human vein	200	40	1

Table 2: summarizes the ResNet-50 model's robust performance in classifying 13 normal histological tissue types, achieving high accuracy (91.54%) and balanced sensitivity and specificity above 91% and 98%, respectively. The positive and negative predictive values indicated strong reliability in identifying true positives and true negatives. Statistically significant results from McNemar's test confirmed the model's superior classification ability compared to EfficientNet-B0.

Sn	Metric	Value (%)	95% Confidence Interval
1	Accuracy	91.54	[90.73 – 92.31]
2	Sensitivity (Recall)	91.71 (Macro	[90.21 – 93.14]
3	Specificity	98.26 (Macro	[97.65 – 98.85]
4	Positive Predictive Value (PPV)	91.36 (Macro	[89.88 – 92.91]
5	Negative Predictive Value (NPV)	98.28 (Macro	[97.62 – 98.89]
6	F1-Score	91.71 (Macro	[90.12 – 93.10]
7	Area Under ROC Curve (AUROC)	98.7	[97.2 – 99.8]
8	McNemar's	p	Statistically significant

93.3%, with an error margin of ±1.8%. Other class-level metrics showed error ranges between ±1.5% and ±2.2%, confirming the statistical reliability and reproducibility of the results as shown in Table 2.

Interpretability and Educational Relevance: The ResNet-50 model demonstrated high classification performance and interpretability through biologically plausible misclassification patterns. These results affirm the model's capacity to mimic expert-level histological judgment and highlight its potential for integration into digital educational platforms. In non-diagnostic academic settings, such tools can standardize histology training, reduce observer variability, and increase scalability, particularly in resource-limited or large-scale teaching environments.

· Accuracy measures the overall proportion of correctly classified images among all the samples.

· Sensitivity (recall) indicates the model's ability to identify true positives for each tissue class correctly.

· Specificity reflects how well the model correctly identifies true negatives and distinguishes each class from the others.

· The Positive Predictive Value (PPV) shows the proportion of positive identifications that were correct (precision).

· The Negative Predictive Value (NPV) represents the proportion of negative identifications that were truly negative.

· F1-Score balances precision and recall, providing a single measure of model accuracy in handling imbalanced data.

· The area under the ROC Curve (AUROC) quantifies the model's overall ability to discriminate between classes across thresholds.

· McNemar's Test evaluates the statistical significance of performance differences between ResNet-50 and a comparator model (EfficientNet-B0).

DISCUSSION

Summary of Key Findings: This study developed and rigorously evaluated a deep learning-based classification pipeline capable of identifying 13 normal human histological tissue types with high accuracy using digitized slides. Utilizing a curated dataset of 3,250 high-resolution annotated images and employing transfer learning via pretrained CNN architectures (ResNet-50, EfficientNet-B0, and MobileNetV2), the best-performing model, ResNet-50, achieved an overall accuracy of 91.54% on the test dataset. Class-wise sensitivity ranged from 80% to 100%, with particularly high scores observed in tissues

such(100%), and bone (95%). The macro-averaged F1-score was 91.71%, and the weighted F1-score reached 91.45%, further confirming the model's robust performance. The statistical significance of the classification differences between the models was evaluated using McNemar's test ($p < 0.05$ for most pairwise comparisons), and 95% confidence intervals were calculated using the Wilson score method, adding rigor to the metric interpretation.

Interpretation of Findings: These findings support the hypothesis that deep learning, particularly CNN-based architectures, by Esteva et a (2021),1) can effectively learn and generalize histological microstructural patterns from a well-balanced dataset [15]. The strong agreement between the predicted and true labels across most tissue types highlights the capacity of CNNs to recognize fine-grained histological features, despite variations in staining intensity and sectioning. Of significance is the statistical validation, which makes these results not only accurate descriptively but also credible. The visualization with error bars/confidence intervals accentuates the stability and generalizability of the model to different histological architectures according to the recommendations for AI-based medical image analysis shown in Table 2.

Comparison with previous studies: Campanella et al. (2019) have focused mainly on validating CNNs in diagnostic histopathology, particularly in cancer detection tasks; our work targets the less investigated, but equally important topic of the classification of normal histological tissues for teaching or anatomical studies [18]. Most previous studies have focused on binary classification (e.g., malignant vs. benign), which does not provide adequate insight into the CNN performance on various types of structurally similar normal tissues. In comparison, we show our approach working for successful multi-class classification over 13 different tissue types, meaning that we can extend the broad application of CNNs to traditional histological education and virtual slide microscopy. This also corresponds with recent work in educational AI for improving anatomy instruction with immersive and automated technologies of Ali Madani et al. (2023) [19].

Unexpected Results: Although high-quality performances were achieved in general, some inter-lobuli misidentifications were also identified among histologically similar tissues, such as white fibrocartilage vs. elastic cartilage and artery vs. vein. These confusions are probably related to histological characteristics, such as the extracellular matrix or the prevalence of elastic fibers. The misclassifications draw attention to the difficulties in determining the cell state, even when histologists are trained, and may be explained by slide preparation artefacts or staining differences. To overcome this issue, ensemble learning or attention mechanisms could be included in future models to make them more suitable for concentrating on discriminative information within complicated tissue matrices.

Theoretical and Practical Contributions:

Theoretically, this study further implies the flexibility of CNNs in complex biomedical image classification, confirming that deep CNNs have the potential for microanatomical structure modeling. In practice, the pipeline has numerous applications: it can have an embeddable implementation as part of a histology e-learning platform, an assistant for remote teaching, and a diagnostic training simulator for students. It also has potential for semi-automatic quality control in histology laboratories. Such a model could democratize access to high-quality histology training and analysis, particularly in less-well-resourced academic institutions, by substantially relieving the manual burden on educators and technicians.

Limitations:

This study is not void of limitations, although it has merits. First, although the dataset was extensive, it was restricted to slides processed and validated at a single academic institution, which may have limited the generalizability of the findings. The variability of staining conditions, imaging resolutions, and sectioning quality when obtained from other sources can all affect the model performance in real-

life applications across institutions. Second, the model performed well in differentiating tissues but not when the tissues were structurally similar, suggesting the potential for architectural or preprocessing enhancements.

Recommendations for Future Research:

Future studies should aim to expand the dataset to include slides from multiple institutions, incorporating variations in staining and sectioning techniques to improve the robustness and generalizability of the model. Integrating attention mechanisms or ensemble models can improve accuracy, particularly in the classification of similar tissue types. Additionally, incorporating model inter pretability tools would be beneficial for educational applications, allowing users to visualize the regions of an image that influence its classification. Exploring the utility of this pipeline in semi-supervised learning scenarios or integrating it with curriculum-based histology modules could further extend its impact.

CONCLUSION

In summary, this study presents a novel and effective deep-learning pipeline for the automated classification of normal histological tissues. By addressing a critical gap in the application of AI to anatomical histology, this study contributes both theoretically and practically to the fields of digital education, biomedical imaging, and computational anatomy. Although certain limitations persist, the findings lay a strong foundation for future advancements in AI-assisted histology education and research.

ACKNOWLEDGEMENTS

I thank and dedicate this research work to my first Anatomy teacher, Dr. Sharadha Kathiresan, who is the source of inspiration to do research.

Conflicts of Interests: None

REFERENCES

[1]. Ball CS. The Early History of the Compound Microscope. Bios. 1966;37(2):51-60.
[2]. Wills M. The Evolution of the Microscope [Internet]. JSTOR Daily. 2018.
[3]. Pallua JD, Brunner A, Zelger B, Schirmer M, Haybaeck J. The future of pathology is digital. Pathol Res Pract. 2020 Sep;216(9):153040. https://doi.org/10.1016/j.prp.2020.153040 PMid:32825928
[4]. A l-Janabi S, Huisman A, Van Diest PJ. Digital pathology: current status and future perspectives. Histopathology. 2012;61(1):1-9. https://doi.org/10.1111/j.1365-2559.2011.03814.x PMid:21477260
[5]. Ahmed AA, Abouzid M, Kaczmarek E. Deep Learning Approaches in Histopathology. Cancers. 2022 Oct 26;14(21):5264. https://doi.org/10.3390/cancers14215264 PMid:36358683 PMCid:PMC9654172
[6]. El-Sherif DM, Abouzid M, Elzarif MT, Ahmed AA, Albakri A, Alshehri MM. Telehealth and Artificial Intelligence Insights into Healthcare during the COVID-19 Pandemic. Healthcare. 2022 Feb 18;10(2):385. https://doi.org/10.3390/healthcare10020385 PMid:35206998 PMCid:PMC8871559
[7]. Fuchs TJ, Buhmann JM. Computational pathology: challenges and promises for tissue analysis. Comput Med Imaging Graph. 2011;35(7-8):515-30. https://doi.org/10.1016/j.compmedimag.2011.02.006 PMid:21481567
[8]. Louis DN, Feldman M, Carter AB, Dighe AS, Pfeifer JD, Bry L, et al. Computational Pathology. Arch Pathol Lab Med. 2016 Jan;140(1):41-50. https://doi.org/10.5858/arpa.2015-0093-SA PMid:26098131 PMCid:PMC4996078
[9]. Kulikowski CA, Shortliffe EH, Currie LM, Elkin PL, Hunter LE, Johnson TR, et al. AMIA Board white paper: definition of biomedical informatics and specification of core competencies for graduate education in the discipline. J Am Med Inform Assoc. 2012;19(6):931-8. https://doi.org/10.1136/amiajnl-2012-001053 PMid:22683918 PMCid:PMC3534470
[10]. Prewitt JMS, Mendelsohn ML. The Analysis Of Cell Images. Annals of the New York Academy of Sciences. 2006 ;128(3):1035-53. https://doi.org/10.1111/j.1749-6632.1965.tb11715.x PMid:5220765
[11]. Zhang Y, Ouyang Z, Zhao H. A statistical framework for data integration through graphical models with application to cancer genomics. The Annals of Applied Statistics. 2017 Mar 1;11(1). https://doi.org/10.1214/16-AOAS998
[12]. Li W, Li J, Sarma KV, Ho KC, Shen S, Knudsen BS, et al. Path R-CNN for Prostate Cancer Diagnosis and Gleason Grading of Histological Images. IEEE Transactions on Medical Imaging. 2019 Apr;38(4):945-54.14. https://doi.org/10.1109/TMI.2018.2875868 PMid:30334752 PMCid:PMC6497079
[13]. LeCun Y, Bagnio Y, Hinton G. Deep Learning. Nature. 2015 May;521(7553):436-44. https://doi.org/10.1038/nature14539 PMid:26017442

[14].Syrykh C, Abreu A, Amara N, Siegfried A, Maisongrosse V, Frenois FX, et al. Accurate diagnosis of lymphoma on whole-slide histopathology images using deep learning. npj Digital Medicine. 2020 May 1;3(1). https://doi.org/10.1038/s41746-020-0272-0 PMid:32377574 PMCid:PMC7195401

[15]. Esteva A, Chou K, Yeung S, Naik N, Madani A, Mottaghi A, et al. Deep learning-enabled medical computer vision. npj Digit Med. 2021 Jan 8;4(1):1-9. https://doi.org/10.1038/s41746-020-00376-2 PMid:33420381 PMCid:PMC7794558

[16]. Coudray N, Ocampo PS, Sakellaropoulos T, Narula N, Snuderl M, Fenyö D, et al. Classification and mutation prediction from non-small cell lung cancer histopathology images using deep learning. Nat Med. 2018 Oct;24(10):1559-67. https://doi.org/10.1038/s41591-018-0177-5 PMid:30224757 PMCid:PMC9847512

[17]. Dercle L, McGale J, Sun S, Marabelle A, Yeh R, Deutsch E, et al. Artificial intelligence and radiomics: fundamentals, applications, and challenges in immunotherapy. J Immunother Cancer. 2022 Sep;10(9):e005292. https://doi.org/10.1136/jitc-2022-005292 PMid:36180071 PMCid:PMC9528623

[18]. Campanella G, Hanna MG, Geneslaw L, Miraflor A, Werneck Krauss Silva V, Busam KJ, et al. Clinical-grade computational pathology using weakly supervised deep learning on whole slide images. Nature Medicine [Internet]. 2019 Aug 1;25(8):1301-9. https://doi.org/10.1038/s41591-019-0508-1 PMid:31308507 PMCid:PMC7418463

[19]. Madani A, Ong JR, Tibrewal A, Mofrad MRK. Deep echocardiography: data-efficient supervised and semi-supervised deep learning towards automated diagnosis of cardiac disease. NPJ Digit Med. 2018;1:59. https://doi.org/10.1038/s41746-018-0065-x PMid:31304338 PMCid:PMC6550282

How to cite this article:

M. Haripriya, Sharad Gavhane, K.Vijayakumar. Automated Classification of Normal Histological Tissues Using Convolution neural network: A ResNet-50-Based Educational Tool. Int J Anat Res 2025;13(3):9306-9313. **DOI:** 10.16965/ijar.2025.201